coatings

MDPI

Article

Multiple Hydrogen-Bonding Assisted Scratch–Healing of Transparent Coatings

Dalius Jucius *, Algirdas Lazauskas and Rimantas Gudaitis

Institute of Materials Science, Kaunas University of Technology, K. Baršausko 59, LT51423 Kaunas, Lithuania; algirdas.lazauskas@ktu.edu (A.L.); rimantas.gudaitis@ktu.lt (R.G.)

* Correspondence: dalius.jucius@ktu.lt; Tel.: +370-37-313-432

Received: 30 October 2019; Accepted: 25 November 2019; Published: 26 November 2019

Abstract: The partial cross-linking reaction of poly(vinyl alcohol) (PVA) by esterification using poly(acrylic acid) (PAA) as a cross-linking agent was performed to obtain a PVA–PAA supramolecular polymer complex. The PVA–PAA coatings with a different molar ratio between hydroxyl and carboxyl groups were prepared to examine scratch–healing ability. These coatings exhibited high optical transparency and excellent scratch–healing properties, which are attributed to considerable amount of free hydroxyl groups at the scratched interfaces to reversibly form multiple hydrogen bonds. Importantly, the PVA–PAA polymer was capable of initiating scratch recovery at temperature of 20 °C and relative humidity (RH) of 40%. Scratches produced on the PVA–PAA polymer coatings with different constant loading in the range of 1.5–2.7 N were healed significantly more rapidly under humid conditions (RH = 99%). Increase of cross-linking temperature also resulted in similar effect but with some reduction of the final scratch healing ratio.

Keywords: poly(vinyl alcohol); poly(acrylic acid); esterification; scratch–healing; transparent; coatings

1. Introduction

In recent years, polymers have become an integral part of our daily lives. Replacement of the natural materials with cheaper, lightweight, flexible plastic has enabled rapid development in all fields of engineering including electronics, construction, aviation, drug delivery, and tissue engineering. On the other hand, polymers are inherently susceptible to damage and continuous usage sooner or later results in formation of cracks and surface scratches, which change the appearance and functional properties of the materials [1]. Considering this fact, it is highly desirable to produce polymers capable of repairing themselves. Such self-healing materials may be very beneficial for the fabrication of easy-to-maintain devices with extended lifetime and enhanced reliability.

Self-healing ability has already attracted substantial attention of researchers and industry as conventional polymer repairing methods are not sufficiently effective for healing the tiniest microcracks and scratches [2–4]. So far, two approaches of polymer self-healing have been developed: extrinsic and intrinsic. Extrinsic approach requires inclusion of specific healing agents in the form of microcapsules or vascular networks, whereas intrinsic self-healing relies on reversible chemical bonds or physical interactions [5,6]. The process of external healing is related to the consumption of healing agent and cannot occur again at the same place. Moreover, fabrication of transparent self-healing materials using extrinsic self-healing approach is technically complicated because various inclusions strongly scatter visible light [7]. Therefore, the intrinsic self-healing approach is considered to be preferable for the fabrication of transparent healable polymers without changing the overall performance of materials.

The intrinsic healing can be generally based on either dynamic covalent bonding or reversibility of supramolecular interactions [8,9]. Reversible opening and closing of dynamic covalent bonds can

be obstructed by occurrence of any side reactions modifying the material repair process [10]. Meanwhile, polymers based on supramolecular chemistry can potentially withstand multiple repair cycles without substantial loss of performance [11]. A broad variety of supramolecular interactions can be exploited with the aim to attain controllable dynamics and good mechanical properties of self-healing polymers [12,13]. However, hydrogen bonding is the most extensively used approach to generate supramolecular polymers [14]. Hydrogen bonds are highly directional and combine high strength with excellent reversibility. Hydrogen bonded supramolecular polymers are not colored, and demonstrate higher mechanical strength and faster healing compared to the polymers cross-linked by other noncovalent or dynamic covalent bonds [15,16].

Herein, we designed the supramolecular system based on partially cross-linked poly(vinyl alcohol) (PVA) and poly(acrylic acid) (PAA), which exhibits high optical transparency and efficient scratch–healing properties. The cross-linking reaction was performed via simple and convenient thermal treatment process. The PAA was chosen as a cross-linking agent because it has a functional carboxyl group in monomer unit to react with hydroxyl group of PVA to form strong ester linkage and is characterized by high solubility in water and high miscibility with PVA [17]. After esterification reaction the polymer complex maintained enough free hydroxyl groups at the scratched interfaces to reversibly form multiple hydrogen bonds, thus demonstrating efficient scratch–healing ability. The PVA–PAA coatings with different molar ratio between hydroxyl and carboxyl groups were probed for scratch–healing and the composition showing the best performance was further systematically analyzed. The performed analysis has demonstrated that the particular PVA–PAA polymer holds a great potential as a high-performance transparent material for optoelectronic applications like foldable smartphones and wearable electronic sensors where scratch–healing properties of the transparent protective coatings are more and more desirable.

2. Materials and Methods

2.1. Materials

All reagents and solvents were obtained at the highest purity and used without further purification unless otherwise specified. For instance, poly(vinyl alcohol) (PVA, average M_w = 30000–70000, 87%–90% hydrolyzed) and poly(acrylic acid) (PAA, 35 wt.% in H_2O, average M_w ~250000) were obtained from Sigma-Aldrich (St. Louis, MO, USA). Twenty-seven percent ammonium hydroxide, NH_4OH, and 30% hydrogen peroxide H_2O_2 were obtained from JSC "Eurochemicals" (Vilnius, Lithuania). Ultrapure water with a resistivity higher than 18.2 MΩ/cm at 25 °C was used in all experiments, and was obtained from a Direct-Q® 3 UV water purification system (Merck KGaA, Darmstadt, Germany). Microscope glass slides were obtained from Thermo Fisher Scientific (Budapest, Hungary).

2.2. Preparation of the PVA–PAA Coatings

Prior to the deposition procedure, RCA-1 cleaning solution (six parts ultrapure water, four parts 27% ammonium hydroxide NH_4OH, and one part 30% hydrogen peroxide H_2O_2) was prepared and heated on a hot plate until its boiling point. Microscope glass slides were immersed into this hot solution for 60 min with continued heating and stirring. Afterwards, glass slides were rinsed three times with deionized water and dried under compressed oxygen. The clear colorless viscous mixtures containing PVA and PAA with molar ratio of hydroxyl groups to carboxyl groups in the range of 3:1–1.5:1 were applied on microscope glass slides as a 50 μm thick layer via the Meyer rod coating method. The coatings were left for 30 min in a vacuum drying oven Vacucentre VC50 (SalvisLab, Rotkreuz, Switzerland) at a temperature of 35 °C and pressure of 400 mbar. Finally, the coatings were thermally cross-linked at 150 or 170 °C for 5 min. The partially cross-linked polymer coating was denoted as PVA–PAA.

2.3. Characterization

Scratch testing of PVA–PAA coatings was performed with a custom-made PC controlled scratch testing apparatus (KTU, Kaunas, Lithuania). Schematic diagram of the used scratch tester is available in Figure S1, Supplementary Materials. During the scratch test, the PVA–PAA coatings were scratched (scratch length 10 mm and speed 0.2 mm/s) with a sphero-conical stylus (cone angle 90° and indenter radius 45 μm) applying the constant loading in the range of 1.2–2.7 N. The scratches were performed in air atmosphere (temperature 23 °C and relative humidity 40%). The B-600MET series upright metallurgical microscope (OPTIKA Srl, Ponteranica, Italy) with a c-mount 2560 × 1920 resolution (5.0 Mpixel) camera (Optikam Pro 5LT) was used for the inspection of a scratch track. The optical images of the scratch tracks were converted to grayscale with brightness and contrast levels equalized for each image, respectively, so that the intensity of pixels in unscratched area would be similar for the same section. Scratch track profiles were obtained using a precision surface roughness tester TR200 (SaluTron Messtechnik GmbH, Frechen, Germany).

The Martens hardness (HM) of the PVA–PAA coatings was measured using a FischerScope HM 2000S (Fischer, Achern, Germany) with a Vickers indenter. Hardness tests were carried out at different locations on the sample surface. An average of five measurements was reported as the hardness value.

A Vertex 70 Fourier transform infrared (FTIR) spectrometer (Bruker Optics Inc., Ettlingen, Germany) equipped with a 30Spec (Pike Technologies) specular reflectance accessory having a fixed 30° angle of incidence (3/16″ sampling area mask) was used to record the spectra. The sample was laid face down across the top of the 30Spec accessory and the spectrum of the sample was recorded at a resolution of 4 cm^{-1}. The software OPUS 6.0 (Bruker Optics Inc., Ettlingen, Germany) was used for the baseline correction and normalization of spectra.

Contact angle (CA) measurements were performed at room temperature using the sessile drop method. A droplet of ultrapure water (5 μL) was deposited onto the investigated surface. Optical images of the droplet were recorded with a PC-connected digital camera after 10 s from the dropping and CA measurements were carried out using an active contour method based on B-spline snakes (active contours) [18].

Optical properties of the PVA–PAA coatings were evaluated by measuring ultraviolet-visible (UV-Vis) transmission. Measurements were conducted using a fiber optic UV/VIS/NIR Spectrometer AvaSpec-2048 (Avantes, Apeldoorn, Netherlands) in the wavelength range from 300 to 800 nm, with a resolution of 1.4 nm.

3. Results and Discussion

In order to investigate the scratch–healing ability of PVA–PAA with different compositions, PVA–PAA coatings with 3:1, 2:1, and 1.5:1 molar ratios between hydroxyl and carboxyl groups were prepared as 50 μm thick layers on microscope glass slides via the Meyer rod coating method. After the thermal cross-linking at 150 °C for 5 min, these coatings were used for the scratch testing. Figure 1 shows optical microscope digital photographs of scratch tracks obtained on the coatings with different constant loading as well as corresponding healing process of the scratch after 24 h at a temperature of 20 °C and relative humidity of 40%. A scratch track profile area was used to calculate a scratch–healing ratio (S_r) of PVA–PAA coatings in Equation (1):

$$S_r = \frac{A_1 - A_2}{A_1} \times 100\%, \quad (1)$$

where A_1 stands for scratch track profile area after scratch, while A_2—scratch track profile area after healing. As evident from Figure 1, all the tested coatings, regardless of particular composition, demonstrated the ability to heal surface scratches. Scratch healing ratio for the scratches made at 1.8 and 2.7 N loading was at least 50%. PVA–PAA polymer coatings prepared with a molar ratio between hydroxyl and carboxyl groups of 1.5:1 (Figure 1c_1–c_4) exhibited the best scratch–healing performance. For these coatings, scratch tracks obtained with the constant loading in the range of 1.2–1.8 N were almost completely healed with S_r in the range of 98.9%–99.2 %. This efficient intrinsic

scratch–healing of the particular coating composition is attributed to considerable amount of free hydroxyl groups at the scratched interfaces to reversibly form multiple hydrogen bonds with sufficient molecular chain mobility present [19–21]. Based on these scratch-testing results, the PVA–PAA polymer coatings prepared with molar ratio between hydroxyl and carboxyl groups of 1.5:1 were selected for further systematic analysis.

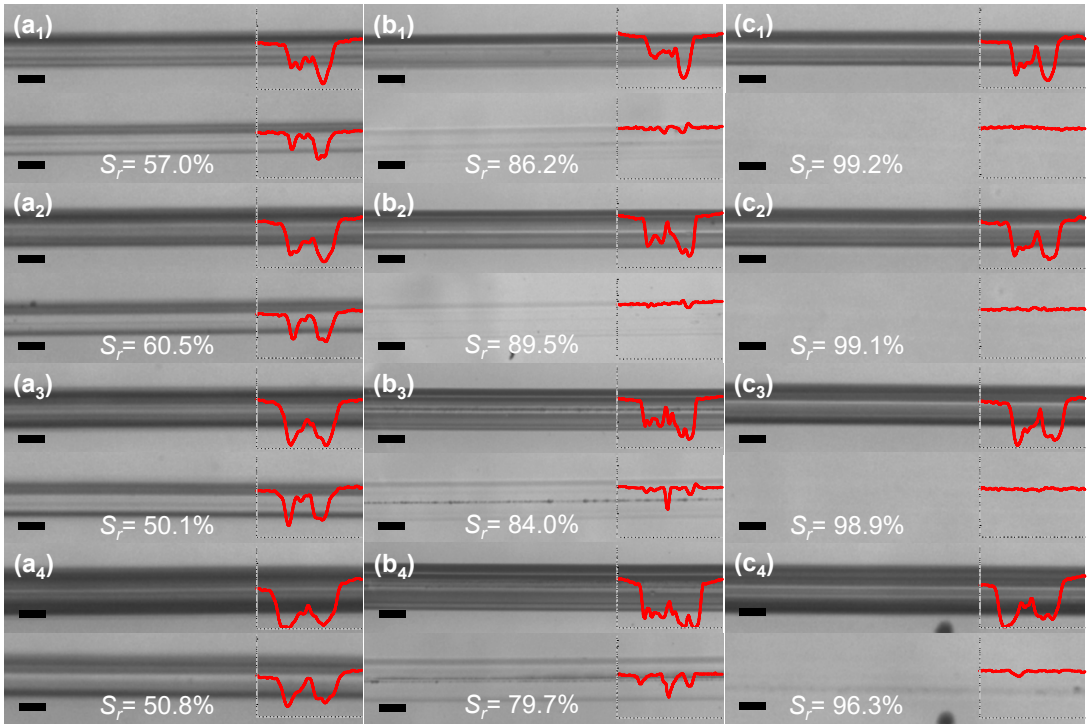

Figure 1. Scratch–healing of the partially cross-linked at 150 °C for 5 min PVA–PAA polymer coatings, with the scratch–healing ratio S_r calculated according to Equation (1). Optical microscope digital photographs show characteristic scratch track sections before and after 24 h at a temperature of 20 °C and relative humidity (RH) of 40% for coatings prepared with molar ratio between hydroxyl and carboxyl groups (**a**1–**a**4) 3:1, (**b**1–**b**4) 2:1, and (**c**1–**c**4) 1.5:1. Subscripts 1–4 indicate scratch constant loading of 1.2 N, 1.5 N, 1.8 N, and 2.7 N, respectively. Insets show characteristic scratch track profiles. Mark size on the bottom left of each digital photograph is 50 μm.

In another scratch-testing instance, the temperature was maintained constant while RH was increased to 99%. Figure 2 shows optical microscope digital photographs of scratch tracks obtained on the coatings (molar ratio between hydroxyl and carboxyl groups of 1.5:1) with different constant loading as well as corresponding healing process of the scratch after 5, 10, 20, and 30 min, respectively. In contrast to previous scratch-testing conditions (see Figure S2, Supplementary Materials), the increase in RH (from 40% to 99%) resulted in rapid scratch–healing process with S_r values in the range of 95.7%–97.4 % after 30 min for different scratch constant loading (Figure 2a5–c5). Owing to hydrophilic and hygroscopic nature of PVA–PAA coatings, significantly more water molecules were attracted from the surrounding at RH of 99%, which increased the chain diffusion across the scratched interfaces and association of the hydroxyl groups to reform multiple hydrogen bonds, thus resulting in more rapid scratch recovery process.

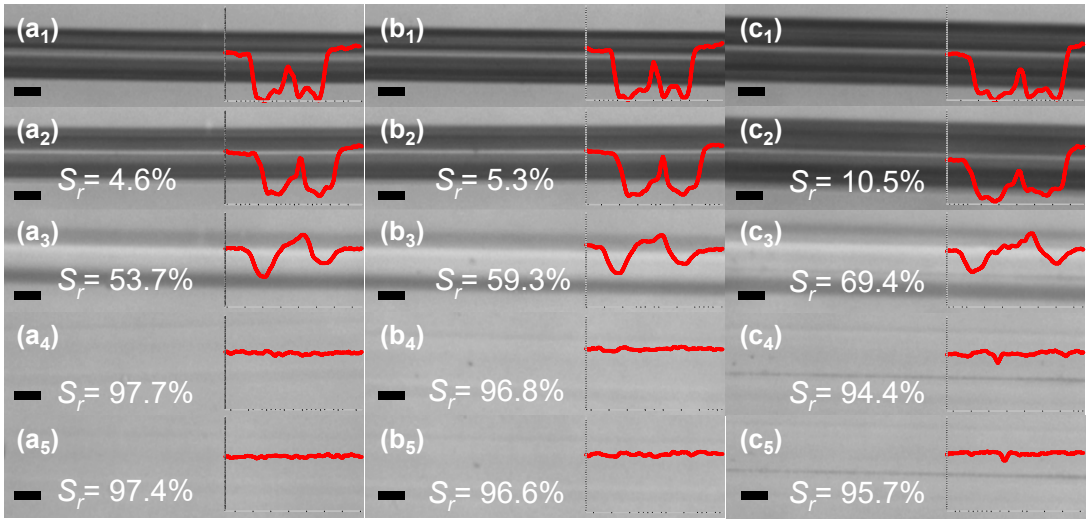

Figure 2. Scratch–healing of the partially cross-linked at 150 °C for 5 min PVA–PAA polymer coatings (molar ratio between hydroxyl and carboxyl groups of 1.5:1), with scratch–healing ratio S_r calculated according to Equation (1). The optical microscope digital photographs show characteristic scratch track sections (**a**$_1$-**c**$_1$) before and after (**a**$_2$–**c**$_2$) 5, (**a**$_3$–**c**$_3$) 10, 20 (**a**$_4$–**c**$_4$), and (**a**$_5$–**c**$_5$) 30 min at a temperature of 20 °C and relative humidity (RH) of 99%. Scratch constant loading of (**a**$_1$) 1.5 N, (**b**$_1$) 1.8 N, and (**c**$_1$) 2.7 N. Insets show characteristic scratch track profiles. Mark size on the bottom left of each digital photograph is 50 μm.

Additionally, it was observed that under high RH conditions the PVA–PAA polymer coatings undergo surface morphological changes with time, leading to the formation of the cellular-like structures (Figure 3). The formation of these structures is attributed to the dominant phase separation of uncross-linked polymer fraction, mainly driven by nucleation-and-growth mechanism [22]. No such morphological changes of PVA–PAA polymer coatings were observed when the cross-linking temperature was increased from 150 to 170 °C, which indicates that higher number of the cross-linking sites was achieved by esterification, in good agreement with [17]. The Martens hardness of the PVA–PAA coatings after thermal cross-linking at 150 and 170 °C was equal to 287 ± 4 N/mm² and 316 ± 5 N/mm², respectively. Figure 4 shows optical microscope digital photographs of scratch tracks obtained on the coatings, thermally cross-linked at 170 °C for 5 min (molar ratio between hydroxyl and carboxyl groups of 1.5:1), with different constant loading as well as corresponding healing process of the scratch after 5, 10, 20, and 30 min, respectively. In contrast to PVA–PAA polymer coatings cross-linked at 150 °C, different scratch–healing manner was observed in this case—the main healing process at a temperature of 20 °C and RH of 99% proceeded during 5 min with S_r values in the range of 92.8%–99.1% for different scratch constant loading (Figure 4a$_1$–c$_1$). After that, no significant changes in scratch recovery were observed. A much faster healing process can be associated with the increased stiffness of PVA–PAA polymer network cross-linked at 170 °C resulting in lesser lateral dimensions of the initial scratches and enhanced delayed elasticity in the high humidity environment. On the other hand, scratch healing ratios for the scratches produced with a constant loading of 1.8 and 2.7 N after 30 min in humid environment did not exceed 93.6% and 92.5%, respectively, and were by ~3% lower compared to the coatings cross-linked at 150 °C. This is the outcome of decrease in the number of free hydroxyl groups at the scratched interfaces to reversibly form multiple hydrogen bonds. Nevertheless, the results obtained were very promising as the scratch recovery process proceeded much faster as compared to the PVA–PAA polymer coatings cross-linked at 150 °C and also relatively high S_r values were obtained.

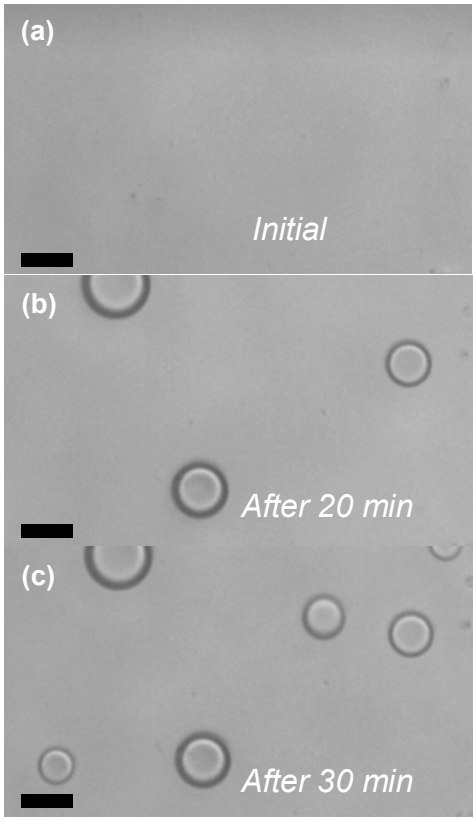

Figure 3. Optical microscope digital photographs of PVA–PAA morphological changes occurring with time at relative humidity (RH) of 99%, leading to the formation of the cellular-like structures – (a) initial, after (b) 20 and (c) 30 min. Mark size on the bottom left of each digital photograph is 50 μm.

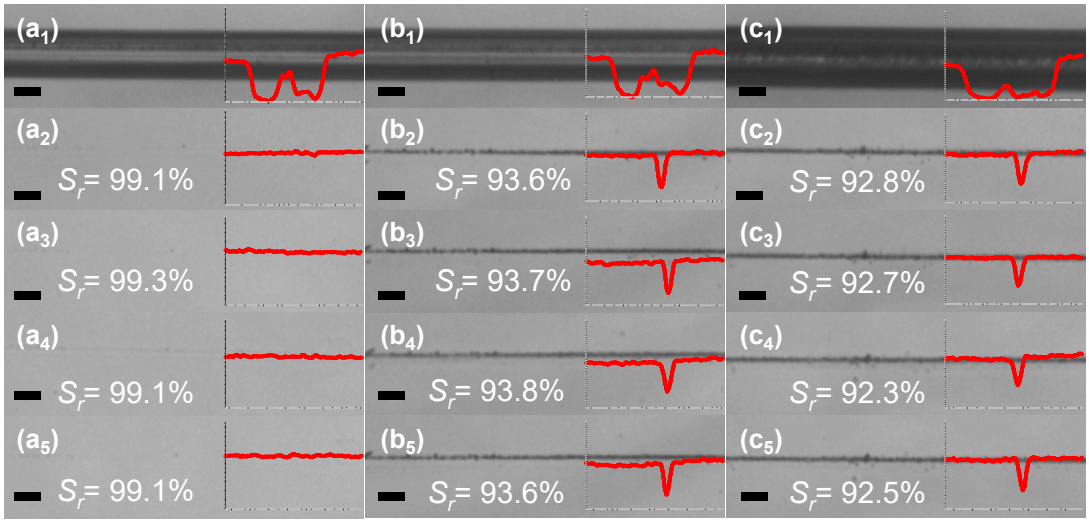

Figure 4. Scratch–healing of the partially cross-linked at 170 °C for 5 min PVA–PAA polymer coatings (molar ratio between hydroxyl and carboxyl groups of 1.5:1), with scratch–healing ratio S_r calculated according to Equation (1). Optical microscope digital photographs show characteristic scratch track sections (**a**1–**c**1) before and after (**a**2–**c**2) 5, (**a**3–**c**3) 10, 20 (**a**4–**c**4), and (**a**5–**c**5) 30 min at temperature of 20 °C and relative humidity (RH) of 99 %. Scratch constant loading of (**a**1) 1.5 N, (**b**1) 1.8 N, and (**c**1) 2.7 N. Insets show characteristic scratch track profiles. Mark size on the bottom left of each digital photograph is 50 μm.

In order to further quantify our results, functional group analysis using FTIR spectroscopy was performed. First of all, FTIR spectra of pure PVA and PAA coatings annealed at 150° C for 5 min were recorded for reference purposes. These spectra were typical of the most common annealed PVA and PAA spectra, and had characteristic peaks of O–H, C–H, C=O, and C-O absorption (see Figure S3, Supplementary Materials). Secondly, we have recorded FTIR spectra of the partially cross-linked PVA–PAA coatings. Figure 5 presents characteristic FTIR spectra of the PVA–PAA coatings with a molar ratio between hydroxyl and carboxyl groups of 1.5:1 cross-linked at 150 and 170 °C for 5 min. In the range from 1500 to 3800 cm^{-1} (Figure 5a), the broad absorption band from 2300 to 3650 cm^{-1} can be assigned to overlapping H–O–H, –OH, and C–H stretching vibrations, while weaker bands at 1745 and 1542 cm^{-1} represent C=O stretching and COO- asymmetric stretching modes [17,23]. For the coatings cross-linked at 170 °C, relative absorbance at 3590 cm^{-1} is smaller due to the lesser absorption of water molecules into the polymer network. Moreover, absorption peaks at 2958, 1746, and 1542 cm^{-1} become narrower and more expressed thus confirming reduction of the disorder in stiffer polymer networks with increased cross-linking density. In the spectral range from 550 to 1250 cm^{-1} (Figure 5b), peaks at 1166, 1056, 1002, 925, and 767 cm^{-1} can be associated with C–O stretching, O–H bending, and $–CH_2–$ stretching [24–26]. Absorption band at 1056 cm^{-1} is a result of anhydride formation upon heating of PAA, whereas the band at 1002 cm^{-1} is an indication of C–O–C ester vibration [27]. In our case, the band at 1002 cm^{-1} becomes significantly stronger after cross-linking of the polymer at 170 °C. At the same time decreased absorption due to O–H bending vibrations at 925 cm^{-1}. These changes confirm esterification reaction between carboxylic acid groups in PAA and hydroxyl groups in PVA.

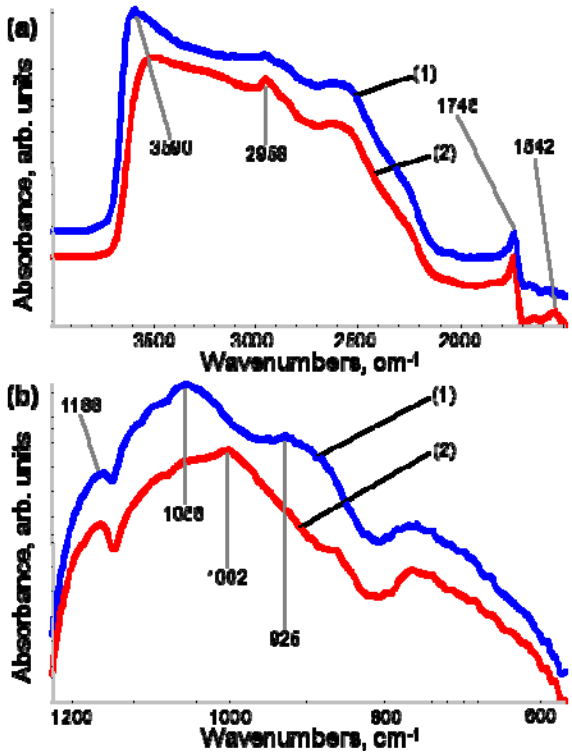

Figure 5. Characteristic FTIR spectra of the PVA–PAA coatings cross-linked at (1) 150 and (2) 170 °C for 5 min (molar ratio between hydroxyl and carboxyl groups of 1.5:1). FTIR spectra presented in two wavenumber ranges: (**a**) 1500 to 3800 cm^{-1} and (**b**) 550 to 1250 cm^{-1}.

Figure 6 shows 5 µL water droplets on the PVA–PAA polymer coatings cross-linked at 150 °C and 170 °C for 5 min with CA indicated. As expected, the PVA–PAA polymer coatings exhibited hydrophilic property with CA values of 45° and 50° for cross-linking temperature of 150 and 170 °C,

respectively. The slight increase of CA in Figure 6b is a result of lower concentration of hydroxyl groups on the surface of PVA–PAA polymer coating cross-linked at 170 °C, in line with the results of scratch-testing and FTIR functional group analysis.

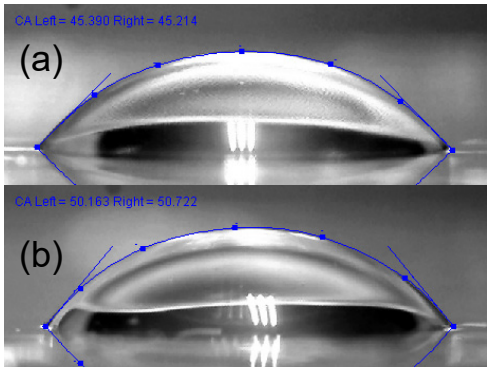

Figure 6. Water droplets on the PVA–PAA polymer coatings cross-linked at (**a**) 150 °C and (**b**) 170 °C for 5 min with the contact angle (CA) indicated.

The UV-Vis transmission spectra of bare and PVA–PAA polymer-coated microscope glass slides are shown in Figure 7. Only a slight decrease in transmittance of wavelengths in the range of 380–800 nm was observed for PVA–PAA coatings as compared with the bare microscope glass, thus both the coatings can be considered highly transparent for visible light. Furthermore, PVA–PAA polymer coatings cross-linked at 170 °C exhibited lower UV transmittance in the range of 300–380 nm. Thus they could be useful for the extra filtering of near-UV light generated by optoelectronic devices.

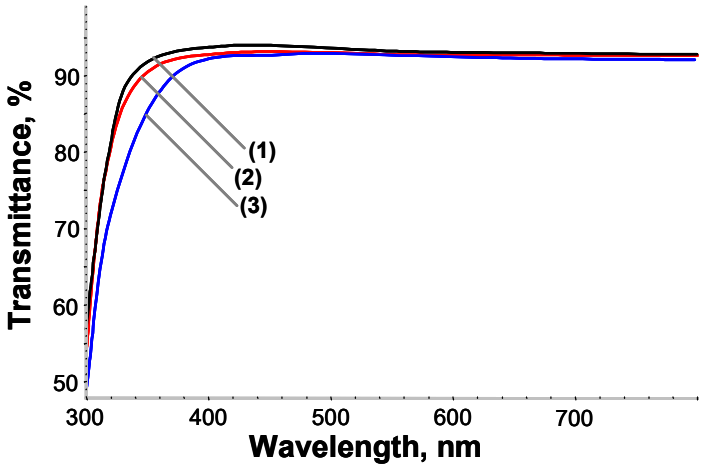

Figure 7. Characteristic UV-Vis transmission spectra of (1) bare and PVA–PAA polymer-coated microscope glass slides with coatings cross-linked for 5 min at (2) 150 °C and (3) 170 °C.

4. Conclusions

The partial cross-linking reaction of PVA by esterification using PAA as a cross-linking agent was performed via simple and convenient thermal treatment process to obtain PVA–PAA supramolecular polymer coatings. It was found that the molar ratio of the hydroxyl groups of PVA to the carboxyl groups of PAA played an essential role in scratch–healing efficiency. After 24 h at a temperature of 20 °C and RH of 40%, the PVA–PAA polymer coatings prepared with a molar ratio between hydroxyl and carboxyl groups of 1.5:1 exhibited the best scratch–healing performance with S_r in the range of 98.9%–99.2% for the scratch tracks obtained with the constant loading in the range of 1.2–1.8 N. This efficient intrinsic scratch–healing of the particular coating composition was

attributed to the considerable amount of free hydroxyl groups at the scratched interfaces to reversibly form multiple hydrogen bonds with sufficient molecular chain mobility present. The increase in RH from 40% to 99% resulted in a more rapid scratch–healing process with S_r values in the range of 95.7%–97.4 % for different scratch constant loading after 30 min of healing. It was observed that under high RH conditions the PVA–PAA polymer coatings cross-linked at 150 °C underwent surface morphological changes with time, leading to the formation of the cellular-like structures. No such morphological changes of PVA–PAA polymer coatings were observed when the cross-linking temperature was increased from 150 to 170 °C, which was attributed to the higher number of the cross-linking sites achieved by esterification. Coatings cross-linked at 170 °C exhibited much faster healing process, which was associated with increased stiffness of PVA–PAA polymer network resulting in lesser lateral dimensions of the initial scratches and enhanced delayed elasticity in the high humidity environment. For these coatings, S_r ratios for the scratches produced with constant loading of 1.8 N and 2.7 N after 30 min in humid environment did not exceed 93.6% and 92.5%, respectively, and were by ~3% lower compared to the coatings cross-linked at 150 °C. FTIR analysis had confirmed the more rapid esterification reaction between carboxylic acid groups in PAA and hydroxyl groups in PVA at 170 °C. The PVA–PAA polymer coatings were found to be hydrophilic and exhibited high transmittance in the visible spectrum. So, these polyfunctional coatings could find application as a high-performance material for optoelectronic applications.

Supplementary Materials: The following are available online at www.mdpi.com/xxx/s1, Figure S1: Schematic diagram of used scratch tester, Figure S2: Scratch–healing of the partially cross-linked at 150 °C for 5 min PVA–PAA polymer coatings with molar ratio between hydroxyl and carboxyl groups of 1.5:1 after 30 min at temperature of 20 °C and relative humidity (RH) of 40%, Figure S3: FTIR spectra of pure (a) PVA and (b) PAA coatings annealed at 150 °C for 5 min.

Author Contributions: Conceptualization, A.L. and D.J.; Methodology, A.L. and D.J.; Validation, A.L. and D.J.; Formal Analysis, A.L. and D.J.; Investigation, A.L., D.J. and R.G.; Resources, A.L.; Writing—Original Draft Preparation, A.L. and D.J.; Writing—Review and Editing, A.L. and D.J.; Visualization, A.L.; Supervision, A.L.; Project Administration, A.L.; Funding Acquisition, A.L.

Funding: This research was funded by the European Social Fund under the No 09.3.3-LMT-K-712-01 "Improvement of researchers' qualification by implementing world-class R&D projects" measure. Grant No. 09.3.3-LMT-K-712-01-0074.

Acknowledgments: A special thanks goes to project members Valentinas Baltrušaitis, Viktoras Grigaliūnas, Asta Guobienė, Brigita Abakevičienė, Igoris Prosyčevas, Mindaugas Andrulevičius and Simas Račkauskas from Kaunas University of Technology for technical assistance.

Conflicts of Interest: The authors declare no conflict of interest.

References

1. Naebe, M.; Abolhasani, M.M.; Khayyam, H.; Amini, A.; Fox, B. Crack damage in polymers and composites: A review. *Polym. Rev.* **2016**, *56*, 31–69.
2. Geitner, R.; Legesse, F.B.; Kuhl, N.; Bocklitz, T.W.; Zechel, S.; Vitz, J.; Hager, M.; Schubert, U.S.; Dietzek, B.; Schmitt, M. Do You Get What You See? Understanding Molecular Self-Healing. *Chem. Eur. J.* **2018**, *24*, 2493–2502.
3. Wu, D.Y.; Meure, S.; Solomon, D. Self-healing polymeric materials: A review of recent developments. *Prog. Polym. Sci.* **2008**, *33*, 479–522.
4. Huynh, T.P.; Sonar, P.; Haick, H. Advanced materials for use in soft self-healing devices. *Adv. Mater.* **2017**, *29*, 1604973.
5. An, S.; Lee, M.W.; Yarin, A.L.; Yoon, S.S. A review on corrosion-protective extrinsic self-healing: Comparison of microcapsule-based systems and those based on core-shell vascular networks. *Chem. Eng. J.* **2018**, *344*, 206–220.
6. Bekas, D.; Tsirka, K.; Baltzis, D.; Paipetis, A. Self-healing materials: A review of advances in materials, evaluation, characterization and monitoring techniques. *Compos. Part B: Eng.* **2016**, *87*, 92–119.
7. Wang, X.; Wang, Y.; Bi, S.; Wang, Y.; Chen, X.; Qiu, L.; Sun, J. Optically transparent antibacterial films capable of healing multiple scratches. *Adv. Funct. Mater.* **2014**, *24*, 403–411.

8. Song, M.-M.; Wang, Y.-M.; Liang, X.-Y.; Zhang, X.-Q.; Zhang, S.; Li, B.-J. Functional materials with self-healing properties: A review. *Soft Matter* **2019**, *15*, 6615–6625.
9. Thakur, V.K.; Kessler, M.R. Self-healing polymer nanocomposite materials: A review. *Polymer* **2015**, *69*, 369–383.
10. van Gemert, G.M.; Peeters, J.W.; Söntjens, S.H.; Janssen, H.M.; Bosman, A.W. Self-healing supramolecular polymers in action. *Macromol. Chem. Phys.* **2012**, *213*, 234–242.
11. Hart, L.R.; Harries, J.L.; Greenland, B.W.; Colquhoun, H.M.; Hayes, W. Healable supramolecular polymers. *Polym. Chem.* **2013**, *4*, 4860–4870.
12. Herbst, F.; Döhler, D.; Michael, P.; Binder, W.H. Self-healing polymers via supramolecular forces. *Macromol. Rapid Commun.* **2013**, *34*, 203–220.
13. Neumann, L.N.; Weder, C.; Schrettl, S. Healing of Polymeric Solids by Supramolecular Means. CHIMIA *Int. J. Chem.* **2019**, *73*, 277–282.
14. Yang, L.; Tan, X.; Wang, Z.; Zhang, X. Supramolecular polymers: Historical development, preparation, characterization, and functions. *Chem. Rev.* **2015**, *115*, 7196–7239.
15. Armstrong, G.; Buggy, M. Hydrogen-bonded supramolecular polymers: A literature review. *J. Mater. Sci.* **2005**, *40*, 547–559.
16. Song, P.; Wang, H. High-Performance Polymeric Materials through Hydrogen-Bond Cross-Linking. *Adv. Mater.* **2019**, 1901244, doi:10.1002/adma.201901244.
17. Kumeta, K.; Nagashima, I.; Matsui, S.; Mizoguchi, K. Crosslinking reaction of poly (vinyl alcohol) with poly (acrylic acid) (PAA) by heat treatment: Effect of neutralization of PAA. *J. Appl. Polym. Sci.* **2003**, *90*, 2420–2427.
18. Stalder, A.F.; Kulik, G.; Sage, D.; Barbieri, L.; Hoffmann, P. A snake-based approach to accurate determination of both contact points and contact angles. *Colloids Surf. A* **2006**, *286*, 92–103.
19. Zhang, X.; He, J. Hydrogen-bonding-supported self-healing antifogging thin films. *Sci. Rep.* **2015**, *5*, 9227.
20. Zhang, H.; Xia, H.; Zhao, Y. Poly (vinyl alcohol) hydrogel can autonomously self-heal. *ACS Macro Lett.* **2012**, *1*, 1233–1236.
21. Spoljaric, S.; Salminen, A.; Luong, N.D.; Seppälä, J. Stable, self-healing hydrogels from nanofibrillated cellulose, poly(vinyl alcohol) and borax via reversible crosslinking. *Eur. Polym. J.* **2014**, *56*, 105–117.
22. Su, Y.; Kuo, C.; Wang, D.; Lai, J.; Deratani, A.; Pochat, C.; Bouyer, D. Interplay of mass transfer, phase separation, and membrane morphology in vapor-induced phase separation. *J. Membr. Sci.* **2009**, *338*, 17–28.
23. Mishra, V.; Kumar, R. Graft copolymerization of carboxymethylcellulose: An overview. *Trends Carbohydr. Res.* **2012**, *4*, 1–17.
24. Daniliuc, L.; De Kesel, C.; David, C. Intermolecular interactions in blends of poly(vinyl alcohol) with poly(acrylic acid)—1. FTIR and DSC studies. *Eur. Polym. J.* **1992**, *28*, 1365–1371.
25. Lu, Y.; Wang, D.; Li, T.; Zhao, X.; Cao, Y.; Yang, H.; Duan, Y.Y. Poly(vinyl alcohol)/poly(acrylic acid) hydrogel coatings for improving electrode–neural tissue interface. *Biomaterials* **2009**, *30*, 4143–4151.
26. Yun, J.-K.; Yoo, H.-J.; Kim, H.-D. Preparation and properties of waterborne polyurethane-urea/poly(vinyl alcohol) blends for high water vapor permeable coating materials. *Macromol. Res.* **2007**, *15*, 22–30.
27. Arndt, K.-F.; Richter, A.; Ludwig, S.; Zimmermann, J.; Kressler, J.; Kuckling, D.; Adler, H.-J. Poly(vinyl alcohol)/poly(acrylic acid) hydrogels: FT-IR spectroscopic characterization of crosslinking reaction and work at transition point *Acta Polym.* **1999**, *50*, 383–390.